AIP | Review of Scientific Instruments

Comment on "Calibration-independent measurement of complex permittivity of liquids using a coaxial transmission line" [Rev. Sci. Instrum. 86, 014704 (2015)]

U. C. Hasar and J. J. Barroso

Citation: Review of Scientific Instruments **86**, 077101 (2015); doi: 10.1063/1.4926595
View online: http://dx.doi.org/10.1063/1.4926595
View Table of Contents: http://scitation.aip.org/content/aip/journal/rsi/86/7?ver=pdfcov
Published by the AIP Publishing

Comment on "Calibration-independent measurement of complex permittivity of liquids using a coaxial transmission line" [Rev. Sci. Instrum. 86, 014704 (2015)]

U. C. Hasar[1,2] and J. J. Barroso[3]
[1]*Department of Electrical and Electronics Engineering, Gaziantep University, 27310 Gaziantep, Turkey*
[2]*Center for Research and Application of Nanoscience and Nanoengineering, Ataturk University, 25240 Erzurum, Turkey*
[3]*Associated Plasma Laboratory, National Institute for Space Research, 12227-010 São José dos Campos, SP, Brazil*

(Received 11 March 2015; accepted 29 June 2015; published online 14 July 2015)

In this letter, we comment on the applicability of the derived characteristic equation (Eq. (7)) in a recently published article of Guoxin [Rev. Sci. Instrum. **86**, 014704 (2015)]. To validate our comment, we first derive another characteristic function for determination of complex permittivity of dielectric materials for the configurations considered in the above article using calibration-independent uncorrected S-parameters for transmission-line measurements (coaxial-line, waveguide, free-space, etc). Unlike the characteristic equation in this article, the characteristic equation derived here for determination of the complex permittivity of liquid samples does not require any knowledge about the complex permittivity of plugs, used for holding liquid samples in place. We then performed 3-D full-wave simulations for the measurement configurations presented in Guoxin's article for substantiation of the characteristic equation derived in this letter. © *2015 AIP Publishing LLC*. [http://dx.doi.org/10.1063/1.4926595]

I. INTRODUCTION

In the article,[1] Dr. Guoxin derived a characteristic equation [Eq. (7) along with Eq. (8)], including relative complex permittivity of the plug ε_{rp}, for the determination of relative complex permittivity (ε_{rs}) of a liquid sample using the 2-D Newton-Raphson numerical method.[2] We think that this characteristic equation should not include ε_{rp} since, as shown in this letter, extraction of ε_{rs} depends only on the electromagnetic properties of a reference medium (usually the universally accepted air medium) to be discussed in our letter. We will comment on this point in our letter by first discussing the concept of the reference medium, then deriving a characteristic equation that relies solely on the electromagnetic properties of the sample, and finally validating this characteristic equation for representative cases.

II. THE CONCEPT OF REFERENCE MEDIUM

A typical stratified composite structure is demonstrated in Fig. 1(a) for illustration of the concept of a reference impedance. Here, the composite structure is composed of N cascaded isotropic, linear, and homogeneous layers with different electromagnetic properties and with different lengths. To simplify the analysis, it is assumed that the whole structure extends to infinity in the transverse dimensions (horizontal axis is taken as the longitudinal dimension).

For the analysis of composite materials such as the one in Fig. 1(a), either the transfer (ABCD) matrix technique[3–5] or the wave cascade matrix (WCM) technique[6–23] can be used. Before application of each of these techniques, a linear, isotropic, and homogeneous reference medium with a small length δ can be assumed between each adjacent layer as shown in Fig. 1(b). In line with the theoretical analysis in Ref. 1, in our letter we consider the WCM technique for analysis of the composite structure in Fig. 1(a). Based on this technique, the WCM matrix of each layer (without each reference medium) can be written in terms of scattering (S-) parameters as[1,8,10,16–24]

$$M_k = \frac{1}{S_{21k}} \begin{bmatrix} (S_{12k}S_{21k} - S_{11k}S_{22k}) & S_{11k} \\ -S_{22k} & 1 \end{bmatrix}, \quad k = 1,2,\ldots,N. \tag{1}$$

To be in line with the analysis given in Ref. 1, assuming that each medium in Fig. 1(a) is reflection-symmetric ($S_{11} = S_{22}$) and reciprocal ($S_{12} = S_{21}$), reflection and transmission S-parameters of each medium can be written as

$$S_{11k} = S_{22k} = \frac{\Gamma_k\left(1 - T_k^2\right)}{1 - \Gamma_k^2 T_k^2}, \quad S_{21k} = S_{12k} = \frac{T_k\left(1 - \Gamma_k^2\right)}{1 - \Gamma_k^2 T_k^2}, \tag{2}$$

where

$$\Gamma_k = \frac{\gamma_r - \gamma_k}{\gamma_r + \gamma_k}, \quad T_k = \exp(-\gamma_k L_k). \tag{3}$$

Here, Γ_k and T_k are the (semi-infinite) reflection and propagation terms of each layer, L_k is the length of each layer, and γ_k and γ_r are the propagation constants of each medium and the reference medium, respectively. We want to highlight that the circumstance of reflection asymmetry ($S_{11} \neq S_{22}$)[25,26] and transmission asymmetry (non-reciprocity) ($S_{12} \neq S_{21}$)[27] is encountered in bi-anisotropic and chiral materials, respectively. We also point out that the assumption that each medium in Fig. 1(a) is transmission symmetric ensures that the whole

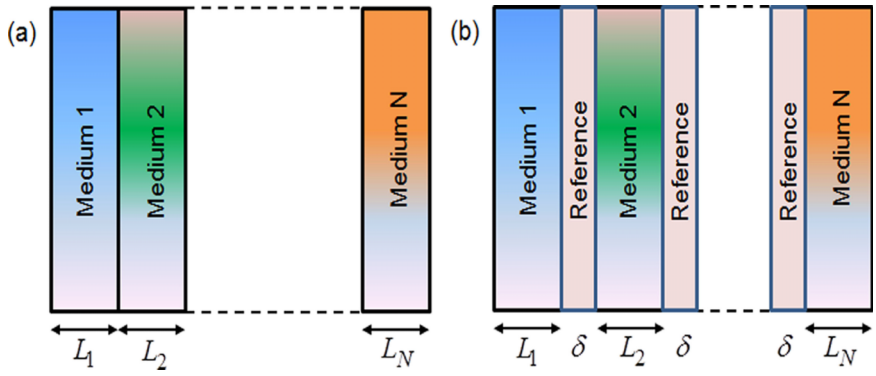

FIG. 1. (a) A stratified composite material with N layers and (b) use of reference medium in between each layer.

structure in Fig. 1(a) is transmission symmetric. Besides, it is not always true to assume that if each layer is reflection asymmetric, the whole structure in Fig. 1(a) will also be reflection asymmetric.[28,29]

In addition to the WCM representation of each medium as given in Eq. (1), we can as well write the WCM representation for each reference medium with length δ in Fig. 1(b). Before continuing further, let us first consider the expressions of reflection and transmission S-parameters of the reference medium. Assuming that the reference medium is reflection symmetric and transmission symmetric, we obtain from Eq. (3) for $\delta = 0$ (to obtain the original structure in Fig. 1(a)),

$$\Gamma_r = 0, \quad T_r = 1, \tag{4}$$

where Γ_r and T_r are the (semi-infinite) reflection coefficient and the propagation factor of the reference medium. Substituting the values of Γ_r and T_r from Eq. (3) into Eqs. (1) and (2) yields

$$S_{11r} = S_{22r} = 0, \quad S_{21r} = S_{12r} = 1, \quad M_r = \begin{bmatrix} 1 & 0 \\ 0 & 1 \end{bmatrix}, \tag{5}$$

where S_{11r}, S_{21r}, S_{12r}, and S_{22r} are the forward and backward reflection and transmission S-parameters of the reference medium and M_r is the WCM representation of the reference medium.

As a result, the overall WCM matrix M_t of the whole structure in Fig. 1(a) can be found by multiplication of the WCM matrices of each medium in Fig. 1(b) as

$$M_t = \prod_{k=1}^{N} M_k, \tag{6}$$

since M_r is a square 2×2 identity matrix for $\delta = 0$.

III. DERIVATION OF A CHARACTERISTIC EQUATION

In this section, we will specialize the general treatment of the WCM matrix analysis in Sec. II to the 3-layer problem shown in Fig. 1 in Ref. 1. In this reference, two three-layer configurations are taken into consideration. In the first one, there is a line section with length l completely filled with air, sandwiched between two plugs (PTFE) with lengths l_{p1} and l_{p2}. The second configuration is identical to the first configuration except that the air line section is replaced with a sample whose electromagnetic properties are to be sought for. Then, using Eq. (6), overall WCM matrices of each configuration in Fig. 1 in Ref. 1 can be written as

$$M_a = T_{m1} T_{ma} T_{m2}, \quad M_s = T_{m1} T_{ms} T_{m2}, \tag{7}$$

where M_a and M_s are the overall WCM matrices of air-filled and sample-filled line sections in Fig. 1 in Ref. 1. Here, T_{m1} and T_{m2} (in general $T_{m1} \neq T_{m2}$) are the WCMs for modeling the transition sections between the vector network analyzer (VNA) and the measurement cell (line section) (more generally, these WCMs denote error (correction) matrices including microwave probes, connectors (launchers), source and load match errors, tracking (frequency) errors, and hardware imperfection of VNA (e.g., VNA IF mixer conversion factor)[6–23]); and T_{ma} and T_{ms} are, respectively, the WCMs when the line section in Fig. 1 in Ref. 1 is empty and loaded with the sample.

Substituting Eqs. (2) and (3) into Eq. (1), expressions of T_{ma} and T_{ms} matrices can be derived as

$$T_{mi} = \frac{1}{(1-\Gamma_i^2)T_i} \begin{bmatrix} T_i^2 - \Gamma_i^2 & \Gamma_i(1-T_i^2) \\ -\Gamma_i(1-T_i^2) & 1-\Gamma_i^2 T_i^2 \end{bmatrix} = T_{\Gamma i} T_{0i} T_{\Gamma i}^{-1}, \tag{8}$$

$$T_{\Gamma i} = \begin{bmatrix} 1 & \Gamma_i \\ \Gamma_i & 1 \end{bmatrix}, \quad T_{0i} = \begin{bmatrix} T_i & 0 \\ 0 & 1/T_i \end{bmatrix}, \quad i = s, a, \tag{9}$$

where Γ_i and T_i are given in Eq. (3).

We note from Eq. (8) and Eq. (3) in Ref. 1 that they are identical to one another if the reference medium is assumed to be the plug medium with electrical permittivity ε_{rp}. However, for most of the cases, the reference medium is assumed to be air[7–23,30,31] for logical reasons. In addition, assuming that the structure in Fig. 1(a) involves just one medium and that it is linear, isotropic, homogeneous, reflection symmetric, and transmission symmetric, then from Eqs. (2) and (3) the S-parameters of this medium will be

$$S_{11} = S_{22} = \frac{\Gamma_1(1-T_1^2)}{1-\Gamma_1^2 T_1^2}, \quad S_{21} = S_{12} = \frac{T_1(1-\Gamma_1^2)}{1-\Gamma_1^2 T_1^2}, \tag{10}$$

where

$$\Gamma_1 = \frac{\gamma_r - \gamma_1}{\gamma_r + \gamma_1}, \quad T_1 = \exp(-\gamma_1 L_1). \tag{11}$$

Equations (10) and (11) will only be correspondingly identical to those used in the literature if the propagation constant of the reference medium γ_r is considered as air (γ_0).[32–40]

To be in line with the expressions in the literature referenced to air (compatible with post-calibration and pre-measurement processes), from now on we assume that the reference medium is assumed to be air. Now, we are at a point to derive a characteristic equation different than the one in Eq. (7) in Ref. 1. Toward this end, multiplying M_s with the inverse of M_a in Eq. (7) we find

$$M_s M_a^{-1} = T_{m1} T_{ms} T_{m2} T_{m2}^{-1} T_{ma}^{-1} T_{m1}^{-1} = T_{m1} T_{ms} T_{ma}^{-1} T_{m1}^{-1}, \tag{12}$$

where the effect of the unknown error WCM matrix T_{m2} on $M_s M_a^{-1}$ is removed.

Besides, from linear algebra, it is well-known that the trace of a square matrix "$\star$" (denoted by $Tr(\star)$) is used to obtain the sum of eigenvalues of this square matrix (sum of diagonal elements in this square matrix) with real or complex entries [determinant of the same matrix "$\star$" (denoted by $\det(\star)$) is used to calculate product of the same eigenvalues]. Thus, the sum of eigenvalues of the multiplied matrix $M_s M_a^{-1}$ in Eq. (12) is equal to

$$Tr(M_s M_a^{-1}) = Tr(T_{m1} T_{ms} T_{ma}^{-1} T_{m1}^{-1}) = Tr(T_{ms} T_{ma}^{-1}), \tag{13}$$

where the last expression in Eq. (13) comes from the similarity-invariance property of Tr. With this operation, it evident that the effect of the other unknown error WCM matrix T_{m1} on $M_s M_a^{-1}$ is removed.

Using Eqs. (8) and (13), we derive the following characteristic equation for the determination of the complex permittivity of a liquid sample with length l:

$$F(\Gamma_s, T_s, T_a) = T_s^2 - \Gamma_s^2 - T_a Tr(M_s M_a^{-1})(1 - \Gamma_s^2) T_s + T_a^2 (1 - \Gamma_s^2 T_s^2) = 0. \tag{14}$$

We note that the derived characteristic equation in Eq. (14) is independent of plug parameters for extraction of electromagnetic properties of the liquid sample. The reason behind this fact is twofold. First, in our formalism we assume that a thin layer of air region (as a reference medium) with length δ is present between each plug and the sample (and the air medium filling the line section), as discussed in Sec. II, and then let the thickness of this air layer approach zero ($\delta = 0$) to realize the measurement configurations in Fig. 1 of Ref. 1. Second, as expected from the property of similarity-invariance of the Tr operation, the plugs should have no effect on extraction of electromagnetic parameters of the sample. This is because the measurement configurations in Fig. 1 in Ref. 1 both contain the same plugs for the same length of line section, which is initially empty and then filled with the sample, and the Tr operation eliminates the effects of error matrices T_{m1} and T_{m2} on this extraction. This situation does not mean that the characteristic equation in Eq. (7) in Ref. 1 is not correct; but, it simply means that air medium, as is usual, instead of plug should have been considered as a reference medium.

When we compare our derived characteristic equation in Eq. (14) with the characteristic equation in (7) in Ref. 1 and with other equations in the literature, we draw the following points. First, considering that the length of the empty air line in Fig. 1 of Ref. 1 reduces to zero ($T_a = 1$), meaning that the configuration in Fig. 1(a) of Ref. 1 reduces to the setup in Fig. 1(a) of Ref. 17, Eq. (14) in this letter simplifies to

$$T_s + \frac{1}{T_s} = Tr(M_s M_a^{-1}) = \frac{\det(M_s + M_a)}{\det(M_a)} - 2. \tag{15}$$

It is seen from Eq. (15) that it is identical to Eq. (8) in Ref. 17. Besides, Eq. (15) in this letter is also equal to Eq. (7) (and Eq. (8)) of Ref. 8 if WCM of a zero-length line section (fully filled with the same unknown sample) is considered ($l_i = 0$ or $l_j = 0$ in the formalism in Ref. 17). We further note that Eq. (15) in this letter is as well in complete agreement with the expressions in Table 1 in Ref. 7. Second, the characteristic equation in Eq. (14) in this letter is much simpler than the characteristic equation in Eq. (7) in Ref. 1.

IV. VALIDATION

To substantiate the derived characteristic equation in Eq. (14) and compare it with the characteristic equation in (7) in Ref. 1, S-parameter simulations of both configurations in Figs. 2(a) and 2(b) were performed by using a commercial 3-D full electromagnetic simulation software (Computer Simulation Technology (CST) Microwave Studio©[41]), which is based on the finite integration technique. In the first configuration, Fig. 2(a), there is an empty waveguide section (airline) with length l = 4.0 mm in between two identical polytetrafluoroethylene (PTFE) plugs with identical lengths l_p = 2.0 mm. In the second configuration, Fig. 2(b), a Plexi-

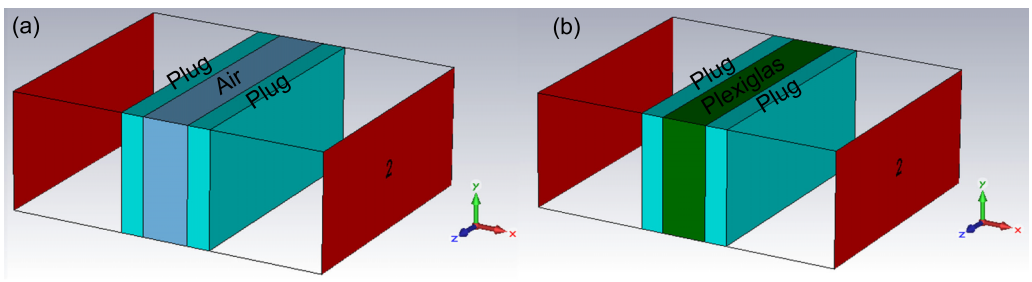

FIG. 2. (a) A waveguide cell with an empty air region with length l between two identical PTFE plugs with lengths l_p and (b) the same cell but loaded with a Plexiglas sample (l).

glas sample with length $l = 4.0$ mm is sandwiched between the same identical PTFE plugs assuming no air gaps [we used Plexiglas sample just for the purpose of demonstration of the correctness of the derived characteristic equation in Eq. (14) instead of a liquid sample]. In simulations, both configurations were positioned within a waveguide section operating at X-band (frequency coverage 8-12 GHz, cutoff frequency $f_c = 6.557$ GHz, broader dimension $a = 22.86$ mm, and narrower dimension $b = 10.16$ mm). Therefore, to simulate such an environment, electric boundary conditions for which tangential components of electric fields are zero ($E_t = 0$) were applied at xy and xz planes for waves propagating in the x direction. To input electromagnetic energy and extract electromagnetic response, we also applied 2 waveguide ports (shown by a red color) at yz planes as seen in Fig. 2. Additionally, in CST simulations, we assumed that over X-band, dielectric properties of the PTFE plugs and the Plexiglas were assumed to be $\varepsilon_{rp} \cong 2.07 - j0.0001$ and $\varepsilon_{rs} \cong 3.60 - j0.035$, respectively. [In Ref. 1, complex permittivity of the PTFE plugs was assumed to be $\varepsilon_{rp} \cong 2.07 - j0.0001$.] We finally note that for waveguide measurements, we considered $\gamma_0 = jk_0\sqrt{1-(f_c/f)^2}$ and $\gamma = jk_0\sqrt{\varepsilon_{rs}-(f_c/f)^2}$ where k_0 is the free-space wavenumber (phase constant) and f is the operating frequency.

Using the boundary conditions discussed above, we obtained forward and backward reflection and transmission S-parameters for both configurations in Figs. 2(a) and 2(b). For example, Figs. 3(a) and 3(b) illustrate the magnitudes of S-parameters obtained from the CST simulations. We next determined M_s and M_a from Eqs. (1) and (2). Then, we calculated the complex permittivity of Plexiglas ε_{rs} using the derived characteristic equation in Eq. (14) in this letter and the characteristic equation in Eq. (7) of Ref. 1. In the calculations, we used the function "fminsearch" of MATLAB© with the same calculation parameters (maximum number of function evaluations allowed as 10^6 with a termination tolerance of 10^{-5}). This function finds the minimum of an unconstrained multivariable function (here, real and imaginary parts of ε_{rs}) in derivative-free manner. Fig. 4(a) demonstrates the frequency dependence of magnitudes of calculated characteristic equations derived in this letter and the one in Ref. 1 by using the

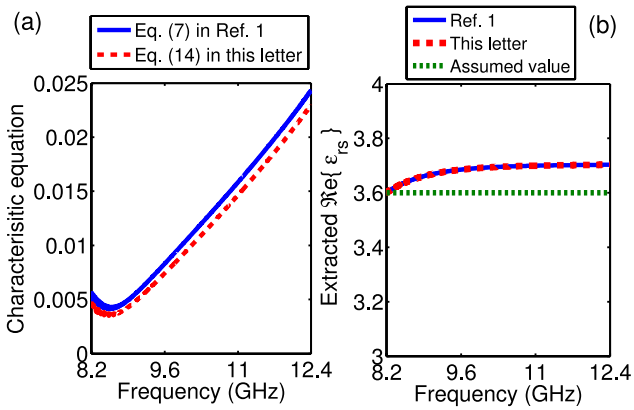

FIG. 4. (a) Dependencies of magnitudes of the characteristic equations in Eq. (14) in this letter and Eq. (7) in Ref. 1 and (b) extracted $\Re e\{\varepsilon_{rs}\}$ of the Plexiglas sample by the characteristic equations in this letter and Ref. 1.

relative complex permittivity of the Plexiglas sample. Besides, Fig. 4(b) illustrates the extracted $\Re e\{\varepsilon_{rs}\}$ of Plexiglas by both characteristic equations in addition to its assumed value (≅3.6). We note from Fig. 4(a) that frequency dependencies of characteristic equations derived in this letter and that in Ref. 1 are almost equal to one another over the whole band. In addition, we notice from Fig. 4(b) that extracted ε_{rs} values of the Plexiglas sample by these characteristic equations are indistinguishable and in good harmony with the assumed ε_{rs} of the Plexiglas sample. The discrepancy between extracted values and the assumed ε_{rs} stems from finite discretization of the CST program and from dispersive characteristics of both the PTFE plugs and the Plexiglas sample in the simulations.[42,43]

We have validated the derived characteristic equation in Eq. (14) by considering the configurations in Figs. 2(a) and 2(b). Nonetheless, these configurations assume that two identical plugs are connected to the sample. In what follows, we will extract the relative complex permittivity of the same Plexiglas sample (with length $L = 4.0$ mm) in between two different dielectric plugs with identical lengths $l_p = 2.0$ mm (non-identical lengths can also be assumed) by using our derived characteristic equation in Eq. (14). The plug on the left side of the Plexiglas sample is still assumed to be the PTFE

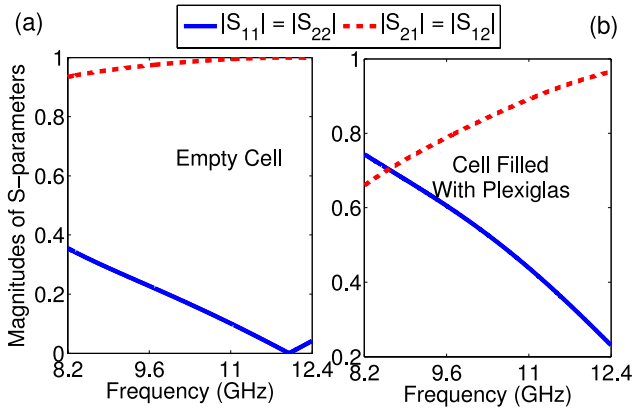

FIG. 3. Magnitudes of simulated S-parameters of (a) empty waveguide cell with length $l = 4.0$ mm between two identical PTFE plugs with lengths $l_p = 2.0$ mm and (b) the same cell filled with a Plexiglas sample ($l = 4.0$ mm).

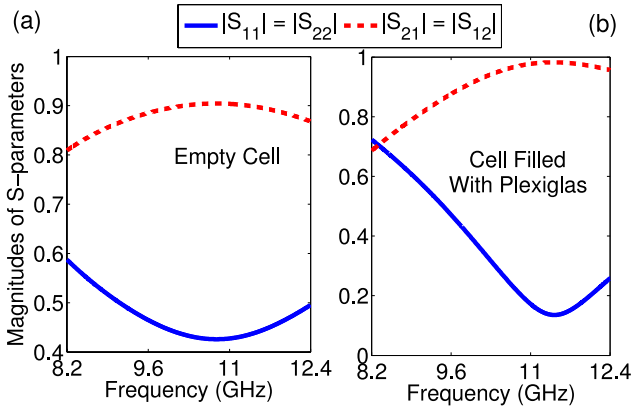

FIG. 5. Magnitudes of simulated S-parameters of (a) the waveguide cell with an empty air region with length $l = 4.0$ mm between a PTFE plug with length $l_p = 2.0$ mm and a lossless FR4 plug with length $l_p = 2.0$ mm and (b) the same cell filled with a Plexiglas sample ($l = 4.0$ mm).

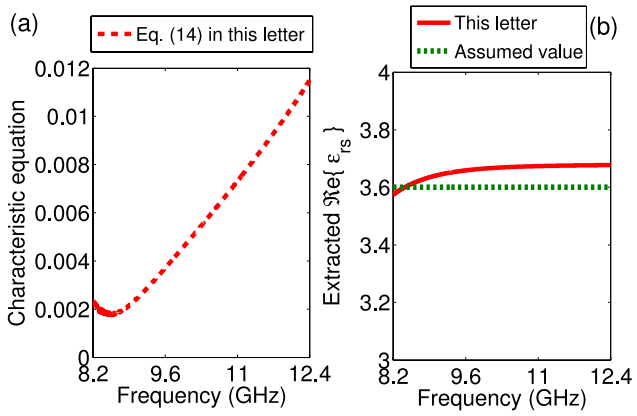

FIG. 6. (a) Dependence of magnitude of the characteristic equation in Eq. (14) and (b) extracted $\Re e\{\varepsilon_r\}$ of the Plexiglas sample by the characteristic equation in Eq. (14).

sample ($\varepsilon_{rp1} \cong 2.07 - j0.0001$) while the plug on the right side of the sample is assumed to be a lossless FR4 material ($\varepsilon_{rp2} \cong 4.3$). Without changing the boundary conditions in our CST Microwave Studio, we have simulated the configurations in Figs. 2(a) and 2(b) with the right-side plug as FR4 dielectric. Figs. 5(a) and 5(b) illustrate the magnitudes of simulated S-parameters for these new configurations.

After obtaining the S-parameters for these new configurations, we then used the function "fminsearch" of MATLAB© with the same calculation parameters (maximum number of function evaluations allowed as 10^6 with a termination tolerance of 10^{-5}) by using the characteristic equation in Eq. (14) in our letter. The dependencies of the characteristic equation in Eq. (14) and the extracted $\Re e\{\varepsilon_{rs}\}$ of the Plexiglas sample over X-band are shown in Figs. 6(a) and 6(b). We note from Figs. 4 and 6 that frequency dependencies of the characteristic equation and the extracted $\Re e\{\varepsilon_{rs}\}$ are, respectively, consistent with one another.

The two different simulation results considered in this letter validate the correctness of the derived characteristic equation in Eq. (14) in our letter and thus demonstrate that there is no need for information about complex permittivity of plugs (identical or non-identical) for extraction of complex permittivity of liquid samples using the configurations in Fig. 1 in Ref. 1.

ACKNOWLEDGMENTS

U. C. Hasar would like to express his thanks to the Scientific and Technological Research Council of Turkey (TUBITAK) under the project Grant No. 112R032 for supporting the finance for the 3-D Electromagnetic simulation program—CST Microwave Studio. He also sends special thanks to the Science Academy of Turkey (the Young Scientists Award in 2014) for supporting his studies.

[1]C. Guoxin, Rev. Sci. Instrum. **86**, 014704 (2015).
[2]W. H. Press, S. A. Teukolsky, W. T. Vetterling, and B. P. Flannery, *Numerical Recipes: The Art of Scientific Computing* (Cambridge University Press, Cambridge, 2007).
[3]U. C. Hasar, I. Y. Ozbek, E. A. Oral, T. Karacali, and H. Efeoglu, Opt. Express **20**, 22208 (2012).
[4]F.-J. Hsieh and W.-C. Wang, J. Appl. Phys. **112**, 064907 (2012).
[5]T. Karacali, U. C. Hasar, I. Y. Ozbek, E. A. Oral, and H. Efeoglu, J. Lightwave Technol. **31**, 295 (2013).
[6]J. Fitzpatrick, Microw. J. **21**, 63 (1978).
[7]J. A. Reynoso-Hernández, IEEE Microw. Wireless Compon. Lett. **13**, 351 (2003).
[8]M. D. Janezic and J. A. Jargon, IEEE Microw. Guid. Wave Lett. **9**, 76 (1999).
[9]I. Huynen, C. Steukers, and F. Duhamel, IEEE Trans. Instrum. Meas. **50**, 1343 (2001).
[10]L. Lanzi, M. Carla, C. M. C. Gambi, and L. Lanzi, Rev. Sci. Instrum. **73**, 3085 (2002).
[11]C. Wan, B. Nauwelaers, W. De Raedt, and M. Van Rossum, IEEE Trans. Microw. Theory Tech. **46**, 1614 (1998).
[12]C. Wan, B. Nauwelaers, and W. De Raedt, IEEE Microw. Guid. Wave Lett. **8**, 58 (1998).
[13]C. Wan, B. Nauwelaers, W. De Raedt, and M. Van Rossum, Electron. Lett. **32**, 1497 (1996).
[14]M.-Q. Lee and S. Nam, IEEE Microw. Guid. Wave Lett. **6**, 168 (1996).
[15]K.-H. Baek, H.-Y. Sung, and W. S. Park, IEEE Microw. Guid. Wave Lett. **5**, 3 (1995).
[16]U. C. Hasar, Electron. Lett. **44**, 585 (2008).
[17]U. C. Hasar, Rev. Sci. Instrum. **79**, 086114 (2008).
[18]U. C. Hasar, IEEE Microw. Wireless Compon. Lett. **18**, 788 (2008).
[19]U. C. Hasar and O. E. Inan, Microw. Opt. Technol. Lett. **51**, 1406 (2009).
[20]U. C. Hasar, IEEE Microw. Wireless Compon. Lett. **19**, 801 (2009).
[21]U. C. Hasar and O. Simsek, J. Phys. D: Appl. Phys. **42**, 075403 (2009).
[22]U. C. Hasar, J. J. Barroso, and M. Ertugrul, J. Electromagn. Waves Appl. **26**, 54 (2012).
[23]U. C. Hasar, G. Buldu, M. Bute, J. J. Barroso, T. Karacali, and M. Ertugrul, AIP Adv. **4**, 107116 (2014).
[24]U. C. Hasar and J. J. Barroso, J. Infrared Milli. Terahertz Waves **33**, 218 (2012).
[25]Z. Li, K. Aydin, and E. Ozbay, Phys. Rev. E **79**, 026610 (2009).
[26]U. C. Hasar, J. J. Barroso, T. Karacali, and M. Ertugrul, AIP Adv. **5**, 017123 (2015).
[27]Z. Li, R. Zhao, T. Koschny, M. Kafesaki, K. B. Alici, E. Colak, H. Caglayan, E. Ozbay, and C. M. Soukoulis, Appl. Phys. Lett. **97**, 081901 (2010).
[28]U. C. Hasar, M. Bute, J. J. Barroso, C. Sabah, Y. Kaya, and M. Ertugrul, J. Opt. Soc. Am. B **31**, 939 (2014).
[29]U. C. Hasar and J. J. Barroso, Opt. Commun. **348**, 13 (2015).
[30]N. J. Farcich, J. Salonen, and P. M. Asbeck, IEEE Trans. Microw. Theory Tech. **56**, 2963 (2008).
[31]Z. H. Jiang and D. H. Werner, Opt. Express **21**, 5594 (2013).
[32]A. M. Nicolson and G. Ross, IEEE Trans. Instrum. Meas. **19**, 377 (1970).
[33]W. B. Weir, Proc. IEEE **62**, 33 (1974).
[34]S. Stuchly and M. Matuszewski, IEEE Trans. Instrum. Meas. **27**, 285 (1978).
[35]J. Baker-Jarvis, E. J. Vanzura, and W. A. Kissick, IEEE Trans. Microw. Theory Tech. **38**, 1096 (1990).
[36]A. H. Boughriet, C. Legrand, and A. Chapoton, IEEE. Trans. Microw. Theory Tech. **45**, 52 (1997).
[37]T. C. Williams, M. A. Stuchly, and P. Saville, IEEE Trans. Microw. Theory Tech. **51**, 1560 (2003).
[38]K. J. Bois, L. F. Handjojo, A. D. Benally, K. Mubarak, and R. Zoughi, IEEE Trans. Instrum. Meas. **48**, 1141 (1999).
[39]U. C. Hasar and C. R. Westgate, IEEE Trans. Microw. Theory Tech. **57**, 471 (2009).
[40]U. C. Hasar, IEEE Trans. Microw. Theory Tech. **58**, 411 (2010).
[41]CST Microwave Studio. Version 2014. Darmstadt (Germany): CST GmbH.
[42]U. C. Hasar, J. J. Barroso, C. Sabah, Y. Kaya, and M. Ertugrul, Opt. Express **20**, 29002 (2012).
[43]U. C. Hasar, J. J. Barroso, G. Buldu, M. Bute, Y. Kaya, T. Karacali, and M. Ertugrul, IEEE J. Sel. Top. Quantum Electron. **21**, 4700211 (2015).